Korean J. Chem. Eng., **26**(4), 1040-1046 (2009)
DOI: 10.2478/s11814-009-0173-z

Performance characterization of direct formic acid fuel cell using porous carbon-supported palladium anode catalysts

Sam Duck Han*, Jae Ho Choi*, Soon Young Noh*, Kunyik Park*, Soo Kyung Yoon, and Young Woo Rhee*,†**

*Department of Chemical Engineering, Chungnam National University, Daejeon 305-764, Korea
**Engineering education innovation center, Ajou University, Suwon 443-749, Korea
(*Received 7 October 2008 • accepted 22 January 2009*)

Abstract−Palladium particles supported on porous carbon of 20 and 50 nm pore diameters were prepared and applied to the direct formic acid fuel cell (DFAFC). Four different anode catalysts with Pd loading of 30 and 50 wt% were synthesized by using impregnation method and the cell performance was investigated with changing experimental variables such as anode catalyst loading, formic acid concentration, operating temperature and oxidation gas. The BET surface areas of 20 nm, 30 wt% and 20 nm, 50 wt% Pd/porous carbon anode catalysts were 135 and 90 m^2/g, respectively. The electro-oxidation of formic acid was examined in terms of cell power density. Based on the same amount of palladium loading with 1.2 or 2 mg/cm^2, the porous carbon-supported palladium catalysts showed higher cell performance than unsupported palladium catalysts. The 20 nm, 50 wt% Pd/porous carbon anode catalyst generated the highest maximum power density of 75.8 mW/cm^2 at 25 °C. Also, the Pd/porous carbon anode catalyst showed less deactivation at the high formic acid concentrations. When the formic acid concentration was increased from 3 to 9 M, the maximum power density was decreased from 75.8 to 40.7 mW/cm^2 at 25 °C. Due to the high activity of Pd/porous carbon catalyst, the cell operating temperature has less effect on DFAFC performance.

Key words: Pd/porous Carbon Catalyst, DFAFC, Anode Catalyst, Formic Acid

INTRODUCTION

The direct methanol fuel cell (DMFC) has been widely studied during the past 20 years and considered as a power source for portable electronic devices such as laptop computers, PDAs, and mobile phones. However, many studies have reported that the DMFC has some disadvantages [1-3]. For example, methanol crossover through the membrane leads to low cell performance. Also, methanol is harmful to health because it is a toxic, evaporable and burnable chemical.

Recently, the advantages of the direct formic acid fuel cell (DFAFC) have been recognized [2,3]. Formic acid is not harmful to humans and is approved by the US Food and Drug Administration (FDA) as a food additive. Also, formic acid has a high theoretical electromotive force (EMF) of 1.45 V as calculated from the Gibbs free energy. This value is higher than that of hydrogen with 1.23 V and methanol with 1.18 V [4,5]. Since formic acid is a strong electrolyte, it is expected to facilitate both electron and proton transfer within fuel cell. The crossover of formic acid through the Nafion® membrane is lower than that of methanol because formic acid partially dissociates in solution, forming a formate anion. The formate anion diffuses very slowly through Nafion® membrane due to the negative charge repulsion between $HCOO^-$ and SO_3^- ion in the Nafion® membrane. On the other hand, methanol dissociates cation diffusing rapidly through Nafion® membrane. Rhee et al. [6] have reported that permeation of formic acid through the Nafion® membrane is much slower than that of methanol. It is two orders of magnitude smaller crossover flux through a Nafion® membrane than methanol. Thus, the energy density of DFAFC can be higher than that of DMFC because DFAFC can be operated at high formic acid concentration.

In many studies, the electro-oxidation of formic acid on the Pt catalyst could undergo through two parallel pathways: a direct pathway and a CO intermediate pathway [7-9]. In the direct pathway, formic acid is directly oxidized to CO_2.

$$HCOOH+Pt^0 \rightarrow CO_2+2H^++2e^- \quad (1)$$

However, in the CO pathway, formic acid is slowly oxidized to CO_2 because formic acid is firstly oxidized to intermediate CO, which is strongly adsorbed on the surface of the catalyst layer.

$$HCOOH+Pt^0 \rightarrow Pt\text{-}CO+H_2O \quad (2)$$

$$Pt^0+H_2O \rightarrow Pt\text{-}OH+H^++e^- \quad (3)$$

$$Pt\text{-}CO+Pt\text{-}OH \rightarrow 2Pt^0+CO_2+H^++e^- \quad (4)$$

The overall reaction is like this.

$$HCOOH \rightarrow CO_2+2H^++2e^- \quad (5)$$

Jiang et al. [10] have shown that the Pt catalyst is not sufficient for formic acid oxidation because the electro-oxidation of formic acid under the Pt catalyst is mainly through the CO pathway. In recent years, many studies have attempted to develop anode catalysts overcoming the CO poisoning effect. It has been demonstrated that Pt-Ru [11], Pt-Pd [12], and Pd-Ir [13] etc. alloys can diminish CO poisoning effect to some extent, but still it is significantly limited by the catalytic activity for formic acid oxidation. Also, the novel metals such as Pt, Pd, and Ru etc. are expensive. Nowadays, in order to reduce the noble metal loading and the system cost, carbon-supported catalysts have been investigated [14-17]. Carbon-supported catalysts are good materials for formic acid oxidation because carbon is cheap conductive support for efficient current collection from

†To whom correspondence should be addressed.
E-mail: ywrhee@cnu.ac.kr

the catalyst layer [14]. The surface of carbon can be coated with highly dispersed noble metal particles. These carbon-supported catalysts lower the noble catalyst loadings while gaining a benefit due to high surface area of carbon.

We investigated the performance characteristics of porous carbon-supported palladium anode catalysts (Pd/porous carbon) in DFAFC. The porous carbon-supported palladium anode catalysts in the DFAFC would reduce palladium loading by increasing palladium efficiency. Both 30 and 50 wt% Pd/porous carbon anode catalysts were synthesized and their performance was characterized in the DFAFC at the various experimental conditions. The effects of pore size, anode catalyst loading, operating temperature and oxidation gas were investigated in terms of cell power density.

EXPERIMENTAL

1. Preparation of Pd/Porous Carbon Anode Catalysts

We prepared four types of Pd/porous carbon anode catalysts. The 30 wt% and 50wt% Pd/porous carbon catalysts with pore size of 20 and 50 nm were prepared by the applied impregnation method. A typical preparation procedure consisted of the following five steps: (1) porous carbon (by Nam et al. [18]) was preconditioned to remove the impurities at 5 M HCl for 12 hours; (2) appropriate amounts of dried porous carbon powder and $PdCl_2$ (Aldrich, A.C.S. Reagent) were dispersed into an appropriate amount of Millipore water; (3) porous carbon solution and $PdCl_2$ solution were mixed and stirred for 24 hours; (4) the mixed solution was impregnated by 0.5 M $NaBH_4$ solution by using a syringe pump at the flow rate of 5 ml/min; (5) finally, the impregnated solution was filtered, and the filtered catalysts cake was rinsed in Millipore water and dried at 80 ºC for 24 hours to make the Pd/porous carbon anode catalyst powder.

The porous carbon and prepared Pd/porous carbon anode catalysts were characterized nitrogen adsorption isotherm, which was measured at liquid nitrogen temperature (77 K) using a Micromeritics ASAP-2010 volumetric adsorption apparatus and high purity nitrogen (99.9999%) was used. Prior to measurement, the porous carbon and Pd/porous carbon anode catalysts were degassed at 423 K for 3 hours in the degas pot of the adsorption analyzer. The BET equation was used to obtain the BET specific surface areas from adsorption data.

2. Single Cell Test

Nafion® 117 (Dupont) was used as a polymer electrolyte membrane. Nafion® 117 membrane was preconditioned prior to fabrication of membrane electrode assembly (MEA) to remove impurities. First, Nafion® 117 membrane was boiled in 5% hydrogen peroxide at 80 ºC. Then, it was boiled in 0.5 M H_2SO_4 at 80 ºC to let protons change to a form of hydrogen ion. Finally, the treated membranes were stored in Millipore water prior to use [6].

The catalyst inks of anode and cathode were prepared by dispersing the catalyst nanoparticles into appropriate amounts of Millipore water and 5 wt% Nafion® solution (EW 1100, Aldrich). To disperse particles, the solution was stirred with an ultrasonicator. Then, catalyst ink of anode was dispersed by dispersing agents (isopropyl alcohol and 1-propanol). Membrane electrolyte assembly (MEA) was made by using a 'direct painting' method. Both the anode and cathode catalyst inks were directly painted onto each side of the Nafion® 117 membrane. The active cell area was 2.25 cm^2 (1.5 cm× 1.5 cm). Also, carbon cloth was used as a fuel and oxidation gas diffusion layer. This carbon cloth diffusion layer was placed on top of the catalyst layer. Especially, carbon cloth of the cathode side was particularly treated with teflon to manage water produced during cell operation.

In this experiment, all of cathode catalysts were Pt black (HISPEC™ 1000, Johnson-Matthey), and the amount of Pt loaded on membrane was 5 mg/cm^2. Five different anode catalysts were investigated in this study: (1) 20 nm, 30 wt% Pd/porous carbon, (2) 20 nm, 50 wt% Pd/porous carbon, (3) 50 nm, 30 wt% Pd/porous carbon, (4) 50 nm, 50 wt% Pd/porous carbon, (5) unsupported Pd black (Aldrich). The anode catalyst loading was changed depending on experimental conditions. 96% A.C.S grade formic acid (Aldrich) was used as a fuel and diluted from 1 to 10 M. The oxidation gas was air or oxygen. Prior to measurement, the MEA was conditioned within the testing fixture at 70 ºC with humidified air and then with formic acid at room temperature for several hours. The anode/cathode flow fields were machined into conductive graphite blocks. Formic acid was supplied to the anode side of the MEA at a flow rate of 1 ml/min; humidified oxidant was supplied to cathode side at a flow rate of 200 ml/min.

The single cell test fixture was designed for use with formic acid. A schematic diagram of the experimental system is shown in Fig. 1. We measured the potential and current density using a D.C electronic loader. Also, we evaluated fuel cell performance in terms of power density according to anode catalyst loading, operating temperature, and oxidant. All experiments were repeated three times to demonstrate reproducibility.

RESULTS AND DISSCUSSION

Table 1 shows the BET surface area of porous carbon and Pd/

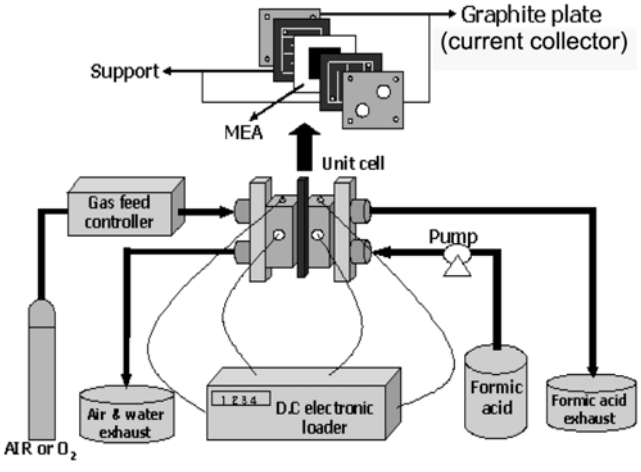

Fig. 1. Schematic diagram of DFAFC unit cell system.

Table 1. BET surface area of porous carbon and Pd/porous carbon

	Porous carbon	30 wt% Pd/porous carbon	50 wt% Pd/porous carbon
20 nm	179 m^2/g	135 m^2/g	90 m^2/g
50 nm	42.7 m^2/g	37 m^2/g	33.5 m^2/g

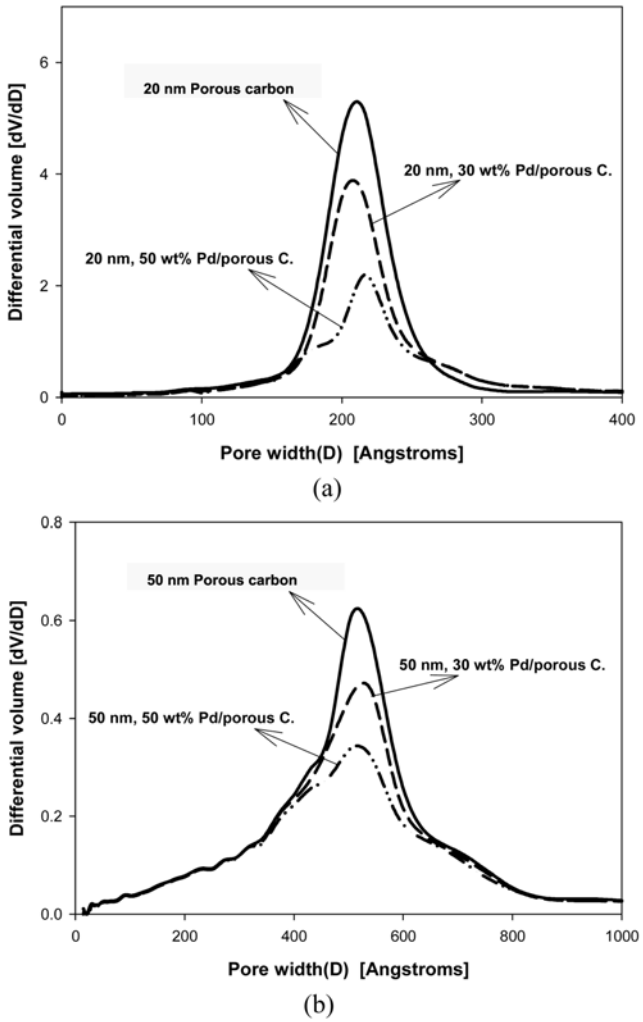

Fig. 2. Pore size distribution curve of porous carbon and prepared anode catalyst.
(a) Porous carbon with 20 nm pore diameter and 20 nm porous carbon-supported palladium catalyst
(b) Porous carbon with 50 nm pore diameter and 50 nm porous carbon-supported palladium catalyst

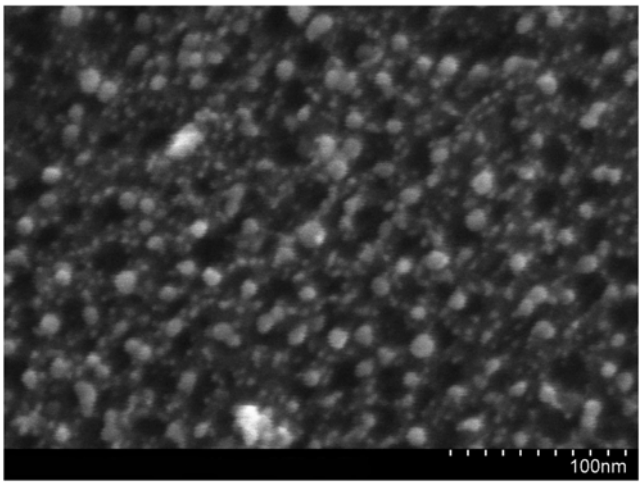

(a) 20 nm, 30 wt% Pd/porous carbon

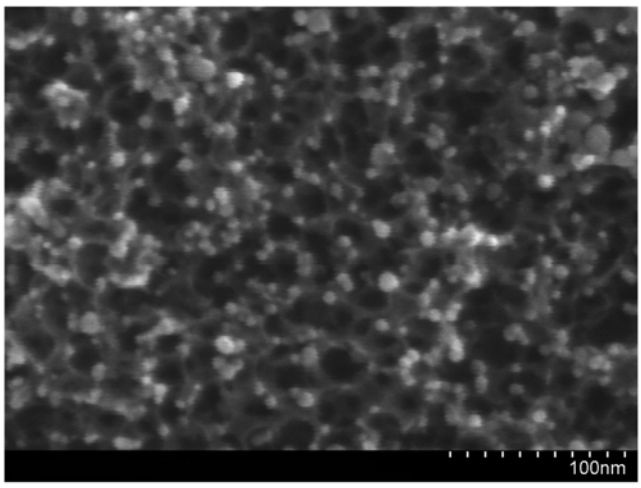

(b) 20 nm, 50 wt% Pd/porous carbon

Fig. 3. SEM images of prepared 20 nm porous carbon-supported palladium anode catalysts.

porous carbon anode catalysts. As expected, 20 nm porous carbon-supported anode catalysts show a higher surface area than 50 nm porous carbon-supported anode catalysts. Also, the prepared 20 nm porous carbon-supported anode catalysts have higher surface areas than commercial Pd black. Especially, the surface area of 20 nm, 30 wt% Pd/porous carbon anode catalyst is 135 m^2/g. BET surface area was decreased as the content of palladium increased. This result implied that the palladium particles filled up the pore when they adsorbed on the pore of the porous carbon. Fig. 2(a) and (b) illustrate the pore size distribution (PSD) curves of the porous carbon and prepared Pd/porous carbon anode catalysts. The maximum peaks appeared at 20 and 50 nm of pore diameters. In both Fig. 2(a) and (b), the intensity of the main peak decreases as the content of palladium increases due to added palladium particles. Also, Figs. 3 and 4 show SEM images of prepared porous carbon-supported palladium anode catalysts, respectively. Fig. 3 shows the (a) 20 nm, 30 wt% Pd/porous carbon and (b) 20 nm, 50 wt% Pd/porous carbon. Fig. 4 show the (a) 50 nm, 30 wt% Pd/porous carbon and (b) 50 nm, 50 wt% Pd/porous carbon. In Figs. 3 and 4, we can confirm that the prepared anode catalysts have a remarkably uniform pore diameter of average 20 nm and 50 nm. Also, the palladium particles were highly dispersed on the porous carbon surface, which indicates that we succeeded in preparing the unimodal types of catalysts that have 20 and 50 nm pore diameters.

Figs. 5 and 6 show the performance comparison of porous carbon-supported Pd and unsupported Pd anode catalysts based on the same amount of palladium loading with 1.2 or 2 mgPd/cm^2. Also, they show the effect of pore size on the performance of fuel cell. Porous carbon-supported Pd anode catalysts show higher cell performance than unsupported Pd catalysts. Also, as the pore size is increased from 20 to 50 nm, the maximum power density is decreased. In Fig. 5, the maximum power density of 20 and 50 nm, 50 wt% Pd/porous carbon anode catalysts (4 mg/cm^2) are 75.8, 47.2 mW/cm^2, respectively. On the other hand, unsupported Pd black of 2 mgPd/cm^2 anode catalyst shows the maximum power density of 27 mW/cm^2. In Fig. 6, the results are the same as those of Fig. 5.

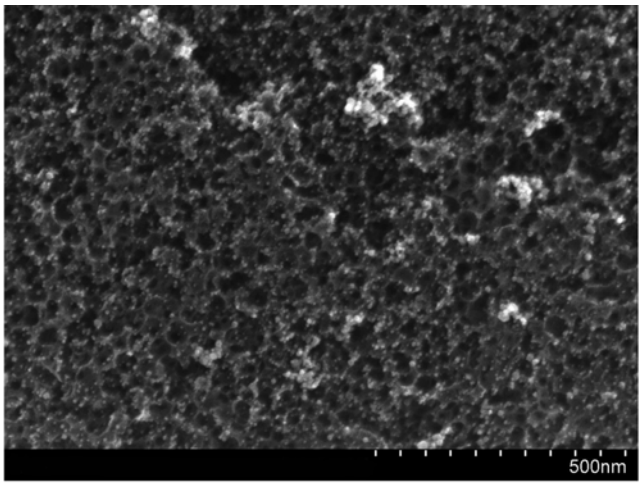

(a) 50 nm, 30 wt% Pd/porous carbon

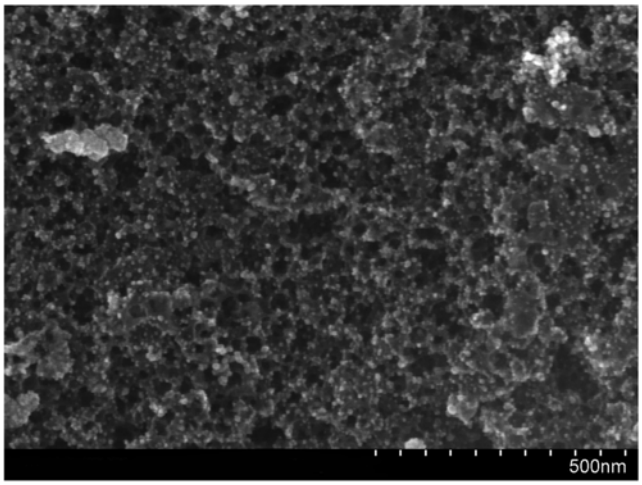

(b) 50 nm, 50 wt% Pd/porous carbon

Fig. 4. SEM images of prepared 50 nm porous carbon-supported palladium anode catalysts.

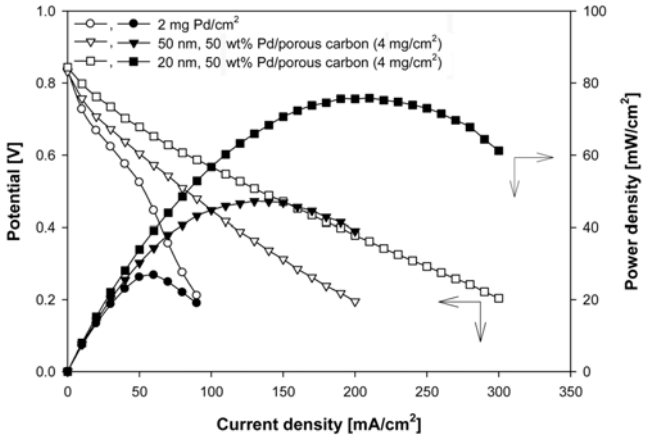

Fig. 5. Performance comparison of porous carbon-supported Pd and unsupported Pd black catalyst with 2 mg Pd/cm² (3 M HCOOH, air, 25 °C).

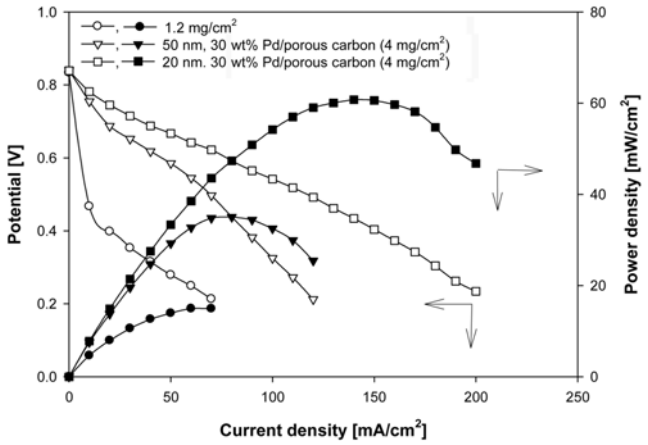

Fig. 6. Performance comparison of porous carbon-supported Pd and unsupported Pd black catalyst with 1.2 mg Pd/cm² (3 M HCOOH, air, 25 °C).

20 and 50 nm 30 wt% Pd/porous carbon anode catalysts generated higher maximum power densities than unsupported Pd black of 1.2 mg/cm². It is believed that the cell performance is significantly increased due to added porous carbon supports. As shown in Table 1, porous carbon-supported palladium anode catalysts have higher BET surface areas than commercial palladium black anode catalyst. Also, 20 nm porous carbon-based anode catalysts show higher cell performance than 50 nm porous carbon based anode catalyst, because 20 nm porous carbon-based anode catalysts have higher surface areas than 50 nm porous carbon-based anode catalysts. So, the high surface area of 20 nm porous carbon will provide a sufficient reaction site for formic acid oxidation. Especially, 20 nm, 50 wt% Pd/porous carbon anode catalyst generated higher performance than

Table 2. The summary of O.C.P., maximum current density and maximum power density with different anode catalysts

Cathode catalyst: 5 mgPt/cm²				
Anode catalyst	O.C.P. (V)	Maximum current density (mA/cm²)	Maximum power density (mW/cm²)	Power density per unit mass of palladium (mW/mgPd)
1.2 mgPd/cm²	0.834	70	15	12.5
2 mgPd/cm²	0.838	100	27	13.5
20 nm, 50 wt% Pd/porous carbon (4 mg/cm²)	0.844	300	75.8	37.9
20 nm, 30 wt% Pd/porous carbon (4 mg/cm²)	0.840	200	60.8	50.7
50 nm, 50 wt% Pd/porous carbon (4 mg/cm²)	0.832	200	47.2	23.6
50 nm, 30 wt% Pd/porous carbon (4 mg/cm²)	0.840	120	35.1	29.3

our previous catalysts such as Pt-Ru [11] and Pt-Pd [12] at similar experimental conditions.

In Table 2, the maximum current densities and maximum power densities are summarized to compare the cell performance. The maximum current density means current measured at the point where electric circuit stops working. The O.C.P. has no difference between Pd/porous carbon and unsupported palladium catalysts. However, the maximum current density and maximum power density are quite different. As shown in Table 2, the cell performance is normalized by the geometrical surface area of catalyst layer with 2.25 cm^2. Although the total power density generated by 30 wt% Pd/porous carbon anode catalyst was lower than that of 50 wt% Pd/porous carbon anode catalyst, the maximum power density per unit mass of palladium metal was much higher than that of 50 wt% Pd/porous carbon anode catalyst. For example, when the cell performance on unit weight of palladium was compared, 20 nm, 30 wt% Pd/porous carbon catalyst generated the maximum power density of 50.7 mW/mgPd. This value is much higher than that of 20 nm, 50 wt% Pd/porous carbon anode catalyst, which is 37.9 mW/mgPd. It implies that even if the added porous carbon provides a high surface area to the catalyst layer, the cell performance is mainly affected by the loading of palladium.

Fig. 7 shows the effect of anode catalyst loading with air as an oxidant. Cathode catalyst loading was 5 mgPt/cm^2 and 20 nm; 50 wt% Pd/porous carbon anode catalyst loadings were 2, 3, 4, and 5 mg/cm^2, respectively. The anode catalyst loading of 4 mg/cm^2 showed the highest cell performance. However, the anode catalyst loading of 2 and 3 mg/cm^2 could not maintain the cell performance up to high current density due to shortage of palladium particle. They have only 1 mg/cm^2 and 1.5 mg/cm^2 of palladium loading. These are low in palladium loading compared to catalyst loading of 4 mg/cm^2 which has palladium loading of 2 mg/cm^2. Interestingly, the cell performance was decreased, though the anode catalyst loading was increased from 4 to 5 mg/cm^2. It is considered that the proton produced by electrochemical reaction cannot transport effectively through Nafion® membrane due to the thick MEA. Namely, the thick MEA interrupts the transfer of proton produced by formic acid oxidation, causing poor performance of the fuel cell.

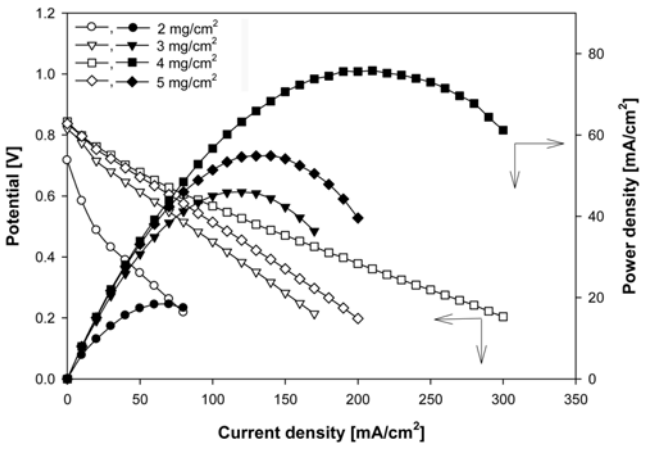

Fig. 7. Effect of anode catalyst loading in DFAFC (Cathode: 5 mgPt/cm^2, anode: 20 nm, 50 wt% Pd/porous carbon, air, 25 °C, 3 M).

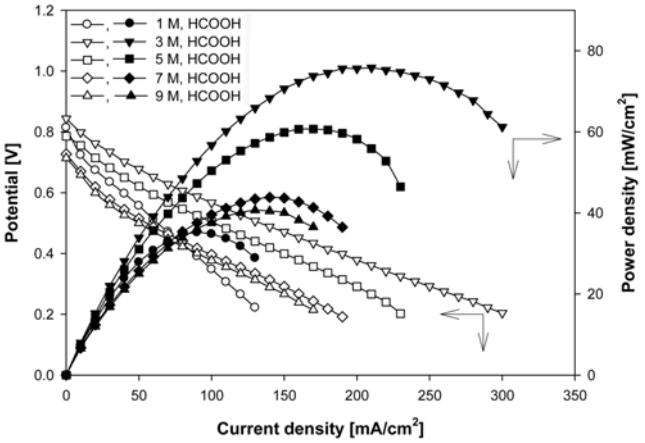

Fig. 8. Effect of formic acid concentration in DFAFC (Cathode: 5 mgPt/cm^2, anode: 20 nm, 50 wt% Pd/porous carbon 4 mg/cm^2, air, 25 °C).

The cell performance at different formic acid concentrations is shown in Fig. 8. Five different formic acid concentrations of 1, 3, 5, 7, and 9 M were examined. We used the new MEA at each experiment to eliminate the effect of operating time because the cell performance was affected by operating time. The OCPs of cell were 0.814, 0.844, 0.786, 0.727, and 0.714 V, respectively, at room temperature. As can be seen in Fig. 8, 3 M formic acid generates the largest maximum power density of 75.8 mW/cm^2. However, 1 M formic acid cannot sustain fuel cell operation at higher current densities because of mass transport limitation. The maximum power densities were significantly decreased when the formic acid concentration was increased from 3 to 9 M. However, the DFAFC can be also well operated with 5 M formic acid. In many studies, the relationship between crossover through the membrane and formic acid concentration had been reported. According to Zhu et al. [19], when the formic acid concentration was increased the crossover current was also increased. They measured the crossover current as the change of formic acid concentration with 1-10 M. When temperature is between 40 and 60 °C, a linear relationship of formic acid crossover with concentration can be observed for all concentrations of formic acid used (1-10 M). If the membrane properties were constant, one would expect a permeation rate proportional to concentration of formic acid. It is also reasonable that lower crossover corresponds to better performance if there is no mass transport limitation. However, a linear relationship between crossover and formic acid concentration is not valid at low temperature (below 30 °C). As a result, by Zhu et al. [19], the crossover phenomenon occurs at lower temperature rather than at higher temperature. Raising temperature will reduce the hydroscopic ability of formic acid because the interaction between molecules decreases.

Fig. 9 shows the effect of oxidation gas, air or oxygen, on the cell performance of DFAFC. The fuel cell was operated at room temperature with 20 nm, 50 wt% Pd/porous carbon anode catalyst loading of 4 mg/cm^2. When oxygen was used as an oxidant, the maximum power density and maximum current density were 103.7 mW/cm^2 and 350 mA/cm^2, respectively. Compared to using the air as an oxidant, the cell performance was increased by about 32%. Namely, the change of oxidant to oxygen enhanced the cell performance of

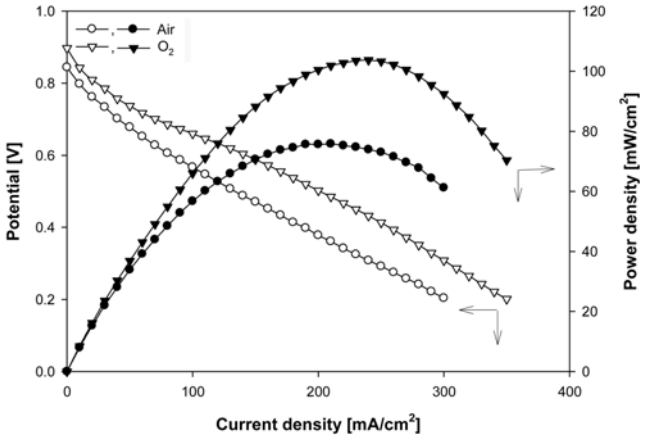

Fig. 9. Effect of oxidation gas in DFAFC performance (Cathode: 5 mgPt/cm^2, anode: 20 nm, 50 wt% Pd/porous carbon 4 mg/cm^2, 3 M, 25 °C).

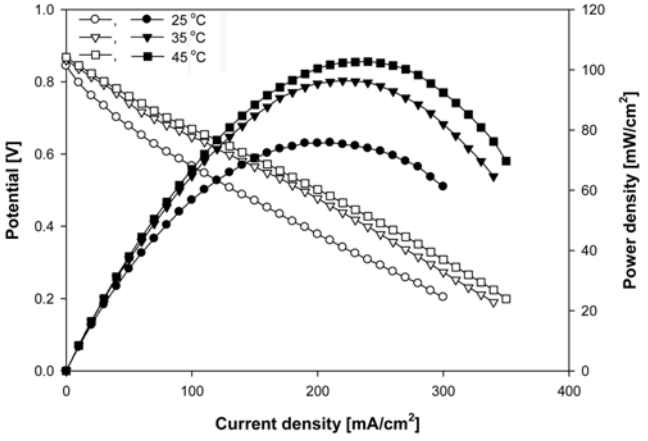

Fig. 10. Effect of operating temperature on the DFAFC performance (Cathode: 5 mgPt/cm^2, anode: 20 nm, 50 wt% Pd/porous carbon 4 mg/cm^2, 3 M, air).

the DFAFC system. Nakagawa et al. [20] reported the effect of oxidant at DMFC system. According to the report, the power density with oxygen feeding was almost twice as high as that with air feeding. The reason of increase on the performance is related to mass transfer of oxygen at the cathode because the mass transfer such as gas diffusion and surface diffusion responds at a relatively high frequency. Since the DFAFC system is very similar to DMFC, the increase of DFAFC performance may be explained by the same reason. An increase of oxygen concentration will make the mass transfer of oxygen easier and faster. So, the faster mass transfer of oxygen will enhance the reaction rate. As a result, the DFAFC with oxygen feeding will show better performance than with air feeding.

Fig. 10 shows the fuel cell performance with an increase of temperature. 20 nm, 50 wt% Pd/porous carbon anode catalyst loading of 4 mg/ cm^2, 3 M formic acid and air were used. When operating temperature was changed from 25 °C to 45 °C, the maximum power density also increased by about 36%. This increase of cell performance can be explained by the Arrhenius equation. According to Arrhenius equation, the reaction rate (k) increased with increasing temperature. As a result, the reaction rate of fuel cell increased, and fuel cell performance increased as well. The fuel cell showed a maximum current density of 350 mA/cm^2 and maximum power density of 103 mW/cm^2 at 45 °C. This value is much higher than that of Pt-Pd anode catalyst (73 mW/cm^2) performed at similar conditions [21]. However, the increasing gap of cell performance decreased with the increase of operating temperature. The fuel cell showed a maximum power density difference of 20.6 mW/cm^2 between 25 and 35 °C. On the other hand, the different of maximum power density was only 6.6 mW/cm^2 between 35 and 45 °C. It is considered that Nafion® membrane demonstrates relatively better proton conductivity at 40-60 °C. So, in this temperature range, the conductivity is the highest in the case of minimum water content. It is mainly related to the movement of the main loop of polymer in Nafion® membrane. The movement of the main loop is the most active in this temperature range so that the proton can be much more easily transported [22]. However, even if the increasing temperature enhances the cell performance by about 36%, this increasing gap is lower than that of Pt-Ru with 72% and Pt-Pd with 44% in DFAFC [21]. It is considered that operating temperature has less effect on the performance due to the high activity of porous carbon-supported palladium catalyst.

CONCLUSIONS

The impregnation method was used to prepare Pd/porous carbon anode catalysts for formic acid electro-oxidation in direct formic acid fuel cell. The prepared Pd/porous carbon-supported Pd and unsupported Pd anode catalysts were characterized in terms of power density. The 20 nm porous carbon-supported palladium anode catalysts had a higher BET surface area than that of 50 nm porous carbon-supported palladium anode catalysts. It was found that high surface area of 20 nm porous carbon based Pd anode catalysts showed excellent results in a fuel cell, while a low surface area of 50 nm porous carbon-based Pd anode catalysts showed much lower activity and deactivation.

The cell performance was mainly affected by anode catalyst loading and formic acid concentration. When the anode catalyst loading was increased from 2 to 4 mg/cm^2 with 3 M formic acid, the cell performance was significantly increased from 18.3 to 75.8 mW/cm^2. Also, when oxygen was supplied to the cathode, the fuel cell generated a maximum power density of 103.7 mW/cm^2 at room temperature. This result corresponds to 27.9 mW/cm^2 improvement when compared to a fuel operated with air at the same condition. The cell operation temperature had little effect on the performance due to the high activity of Pd/porous carbon catalyst. The fuel cell with air feeding generated the maximum power density of 102.7 mW/cm^2 at 45 °C, which corresponds to about 36% enhancement compared to that obtained at 25 °C. It is confirmed that palladium is a good material for formic acid oxidation and Pd/porous carbon anode catalyst is a promising anode catalyst for the DFAFC.

REFERENCES

1. R. Dillon, S. Srinivasan, A. S. Arico and V. Antonucci, *J. Power Sources*, **127**, 112 (2004).
2. S. Ha, B. Adams and R. I. Masel, *J. Power Sources*, **128**, 119 (2004).
3. C. Rice, S. Ha, R. I. Masel and A. Wieckowski, *J. Power Sources*,

115, 229 (2003).
4. S. Ha, C. Rice, R. I. Masel and A. Wieckowski, *J. Power Sources*, **112**, 655 (2002).
5. C. Rice, S. Ha, R. I. Masel, P. Waszczuk, A. Wieckowski and T. Barnard, *J. Power Sources*, **111**, 83 (2002).
6. Y. W. Rhee, S. Ha and R. I. Masel, *J. Power Sources*, **117**, 35 (2003).
7. X. H. Xia and T. Iwasita, *J. Electrochem. Soc*., **140**, 2559 (1993).
8. N. M. Markovic, H. A. Gasteiger, P. N. Ross, X. Jiang, I. Villegas and J. Weaver, *Electrochim. Acta*., **40**, 91 (1995).
9. R. Parsons and T. VanderNoot, *J. Electroanal. Chem*., **257**, 9 (1998).
10. J. Jiang and A. Kucernak, *J. Electroanal. Chem.*, **520**, 64 (2002).
11. J. S. Kim, J. K. Yu, H. S. Lee, J. Y. Kim, Y. C. Kim, J. H. Han, I. H. Oh and Y. W. Rhee, *Korean J. Chem. Eng.*, **22**, 661 (2005).
12. K. H. Kim, J. K. Yu, H. S. Lee, J. H. Choi, S. Y. Noh, S. K. Yoon, C. S. Lee, T. S. Hwang and Y. W. Rhee, *Korean J. Chem. Eng.*, **24**, 518 (2007).
13. X. Wang, Y. Tang, Y. Gao and T. Lu, *J. Power Sources*, **175**, 784 (2008).
14. S. Ha, R. Laesen and R. I. Masel, *J. Power Sources*, **144**, 28 (2005).
15. L. Zhang, Y. Tang, J. Bao, T. Lu and C. Li, *J. Power Sources*, **162**, 177 (2006).
16. S. Yang, X. Zhang, H. Mi and X. Ye, *J. Power Sources*, **175**, 26 (2008).
17. Z. Liu, L. Hong, M. P. Tham, T. H. Lim and H. Jiang, *J. Power Sources*, **161**, 831 (2006).
18. K. D. Nam, T. J. Kim, S. K. Kim, B. R. Lee, D. H. Peck, S. K. Rhu and D. H. Jung, *J. Korean Ind. Eng. Chem*., **17**, 223 (2006).
19. Y. Zhu, S. Ha and R. I. Masel, *J. Power Sources*, **130**, 8 (2004).
20. N. Nakagawa and Y. Xiu, *J. Power Sources*, **118**, 248 (2003).
21. J. K. Yu, H. S. Lee, K. H. Kim, Y. C. Kim, J. H. Han, I. H. Oh and Y. W. Rhee, *Korean Chem. Eng. Res.*, **44**, 314 (2006).
22. P. C. Rieke and N. E. Vanderborgh, *J. Membrane Science*, **32**, 313 (1987).